INTERNATIONAL JOURNAL FOR NUMERICAL METHODS IN FLUIDS
Int. J. Numer. Meth. Fluids 2005; **48**:521–539
Published online 3 March 2005 in Wiley InterScience (www.interscience.wiley.com). DOI: 10.1002/fld.947

Diffusion via splitting and remeshing via merging in vortex methods

Mei-Jiau Huang*,†

Department of Mechanical Engineering, National Taiwan University, Taiwan

SUMMARY

The technique of splitting a fat vortex element (with a core width larger than some threshold) into some thin ones in order to fix the convergence problem of the core-spreading vortex methods is convenient and efficient. In particular, it keeps the method purely Lagrangian. In the present investigation, the splitting process is further viewed as part of the physical diffusion process. A new splitting method in which several weaker child vortices surround a thinned but still strong parent vortex is proposed. It is found that because of the survival of the parent vortex, the error arising from the splitting events can be largely reduced. The computational amount on the other hand is kept reasonably large by merging similar and close-by vortices. The merging scheme designed herein not only involves fewer restrictions but also allows merging vortices of opposite rotations through the viewpoint of remeshing. The validity and accuracy of these techniques, proposed particularly for simulations undergoing lots of splitting and merging events, are verified by successfully simulating the interactions between two Burgers vortices under an external straining field. Copyright © 2005 John Wiley & Sons, Ltd.

KEY WORDS: vortex method; vortex splitting; diffusion; vortex merging; remeshing

1. INTRODUCTION

The discrete vortex method (see Reference [1]) has been developed as a numerical simulator for two-dimensional incompressible inviscid flows. In this method, the convection of packets of vorticity (vortex elements) is tracked. The method can be thus implemented grid free. The compactness of the vorticity field compared to that of the primitive variables also makes the vortex method advantageous, in addition to its exact satisfaction of boundary conditions at infinity for external flows. Viscous effects however are important but difficult to be added in such a Lagrangian approach because of poor evaluation of the Laplacian operator due to scattered, unpredictable distributions of the vortex elements. The most straightforward viscous

*Correspondence to: Mei-Jiau Huang, Department of Mechanical Engineering, National Taiwan University, Taiwan.
†E-mail: mjhuang@ntu.edu.tw

Contract/grant sponsor: National Science Council; contract/grant number: NSC 91-2212-E-002-092

Received 9 September 2004
Revised 15 December 2004
Accepted 20 December 2004

treatment simply uses grid-based finite-difference methods by mapping data between the Eulerian and Lagrangian grids (see Reference [2]). Interpolations are therefore needed in order to evaluate the Laplacian operator and perform mapping, which possibly result in excessive numerical diffusion. Another vortex method using the mapping technique is the diffusing-vortex method first proposed by Lu and Shen [3] and extended later by Lu and Ross [4]. In this method, discretized vortices, located at the mesh points of a fixed grid, always start from the mesh points and move only one time step. To simulate diffusion, each vortex spreads its vorticity in a Gaussian distribution. The new vorticity at each mesh point then defines the new vortex.

Several purely Lagrangian schemes have also been proposed. The core-spreading method was introduced by Leonard [1], in which the core widths of vortex elements grow exactly according to the heat diffusion equation. A localized re-gridding is required nonetheless for a correct convergence to the Navier–Stokes equations [5]. For the sake of simulating diffusion, the random-walk approach proposed by Chorin [6] added a pseudo-random velocity like the Brownian motion to the element velocity. It was shown nonetheless that the scheme converges slowly and provides a low resolution, although it is stable. The particle-strength-exchange scheme (see Reference [7]) redistributes the strength (circulation) among vortex elements to account for diffusion by approximating parts of the governing equations by integral operators. Fishelov [8] proposed to apply the Laplace operator on the convolution of some cut-off function with the delta distribution function. Both methods encounter with difficulties however when the flow becomes strained. Lots of remeshing processes are required in order to maintain a regular distribution of the vortex elements. This increases the computational amount and makes schemes not so perfectly Lagrangian. Instead of approximating the Laplace operator by integral operators, the vortex-redistribution method proposed by Shankar and van Dommelen [9, 10] distributes fractions of circulation of each vortex to its neighbouring vortices within a chosen distance. The fractions are computed by equating the Fourier transforms with some truncated Taylor series of the exactly diffused vorticity and the resulting vorticity after the redistribution. A solution of the redistribution equations however does not necessarily exist. New vortices with zero circulation must be added then until a solution does become possible.

In 1991, Ogami and Akamatsu [11] proposed a method called the diffusion-vortex method in which a diffusion velocity is defined and added to the element velocity to simulate diffusion. The method was improved later by Kempka and Strickland [12], Shintani and Akamatsu [13], Huang [14], as well as Huang and Chen [15]. In spite of having a stronger physical basis and the conservation of circulation on any arbitrary 'diffusion material surface' (a surface which moves at the total velocity of the fluid velocity and the diffusion velocity), the diffusion-vortex method requires many more computations and has a difficulty in evaluating the diffusion velocity when the local vorticity is zero. Moreover, the core widths still generally grow in time. The convergence problem is still existent. For more details of these vortex methods, the readers may be referred to the works of Leonard [16], Anderson and Greengard [17], Gustavson and Sethian [18], Beale *et al.* [19], Cottet and Koumoutsakos [20], and so on.

To fix the convergence problem of the core-spreading vortex methods, Rossi [21] proposed the solution of replacing a too fat vortex element (called a parent vortex) by several thin ones (called child vortices). The strengths and the locations of the child vortices are determined by preserving the total circulation and the second moment of the vorticity about the centre of the parent vortex. The core widths of vortex elements can thus remain small at all times, although the number of computational elements grows terribly rapidly. To control the number,

Rossi then suggested that similar and close-by vortices should be merged into one [22]. These techniques have been employed for a study of monopole and tripole attractors for relaxing vortices [23]. Worry arises however when simulations must undergo very many splitting and merging events such that the so-induced errors may become unacceptable. The motivation of the present study is thus to seek for an improvement of Rossi's techniques.

First, the splitting process may be viewed as a part of the diffusion process. In other words, the circulation is kind of being diffused or thrown away from the parent vortex by generating child vortices. An important issue is that the parent vortex just becomes weaker and should still exist after diffusion. A physically reasonable layout after splitting is thus a weakened and thinned parent vortex surrounded by several child vortices. In the present work, such a splitting method will be proposed and investigated.

Secondly, in Rossi's merging scheme, many criteria are required to judge a success of a merging event. Related computations become useless and wasted if any of these criteria is not fulfilled. Moreover, merging vortex elements of opposite rotations is not considered, which however is not impossible from the viewpoint of remeshing and is necessary for an economic simulator. A modified merging scheme that involves fewer restrictions and allows merging vortices of opposite rotations is therefore desired and designed herein.

This paper is arranged as follows. Leonard's original core-spreading vortex method is reviewed in Section 2.1. The splitting methods of interest are introduced and compared in Section 2.2. Rossi's merging method and the one modified by the author are both discussed in Section 2.3. To demonstrate the validity and accuracy of these newly proposed splitting and merging schemes, they are applied to the simulations of the interactions between two identical Burgers vortices of same or opposite rotations under an external straining field in Section 3. Physical quantities are measured and compared with those obtained from previous investigations [24, 25]. Conclusions are finally given in Section 4.

2. NUMERICAL METHODS

2.1. Core-spreading vortex method

For two-dimensional incompressible Newtonian-fluid flows, the governing equation for vorticity (ω) is

$$\frac{\partial \omega}{\partial t} + u\frac{\partial \omega}{\partial x} + \upsilon\frac{\partial \omega}{\partial y} = \nu\nabla^2\omega \tag{1}$$

where u and υ are the velocity components, and ν is the fluid viscosity. In a vortex method, a vorticity field is composed of vortex elements. If Gaussian vortices are adopted, the vorticity field is written as

$$\omega(\mathbf{x},t) = \sum_{j=1}^{N} \frac{\Gamma_j}{\pi\sigma_j^2} \exp\left(-\frac{|\mathbf{x}-\mathbf{x}_j|^2}{\sigma_j^2}\right) \tag{2}$$

where $\Gamma_j(t)$ is the circulation (strength) of the jth vortex element, distributed mainly within a distance of $\sigma_j(t)$ (core width) from the centre of the element, $\mathbf{x}_j(t)$. Equation (1) is then satisfied by properly selecting $\sigma_j(t)$, $\mathbf{x}_j(t)$, and $\Gamma_j(t)$. In Leonard's core-spreading vortex method, a vortex element preserves its circulation, moves at its central fluid velocity, and

changes its core width in such a way that the diffusion term in Equation (1) is exactly satisfied. In a word,

$$\frac{\mathrm{d}\Gamma_j}{\mathrm{d}t} = 0 \tag{3}$$

$$\frac{\mathrm{d}\mathbf{x}_j}{\mathrm{d}t} = \mathbf{u}(\mathbf{x}_j, t) \tag{4}$$

$$\frac{\mathrm{d}\sigma_j^2}{\mathrm{d}t} = 4v \tag{5}$$

where the velocity components can be evaluated through the Biot–Savart law:

$$u(\mathbf{x}) = -\sum_{j=1}^{N} \frac{\Gamma_j}{2\pi} \frac{(y - y_j)}{|\mathbf{x} - \mathbf{x}_j|^2} \left\{ 1 - \exp\left(-\frac{|\mathbf{x} - \mathbf{x}_j|^2}{\sigma_j^2} \right) \right\} \tag{6}$$

$$v(\mathbf{x}) = \sum_{j=1}^{N} \frac{\Gamma_j}{2\pi} \frac{(x - x_j)}{|\mathbf{x} - \mathbf{x}_j|^2} \left\{ 1 - \exp\left(-\frac{|\mathbf{x} - \mathbf{x}_j|^2}{\sigma_j^2} \right) \right\} \tag{7}$$

Consequently, when substituting Equations (2)–(5) into Equation (1), one finds that the diffusion term is satisfied completely but the convection terms are not [1]. To keep the associated error small, the core widths of the vortex elements must remain small. Equation (5) nonetheless implies that the core widths increase with time and therefore so does the error. This error then leads to an incorrect convergence of the numerical solutions [5].

2.2. *Splitting schemes*

The idea of splitting a fat vortex into several thin ones was firstly proposed by Rossi [21]. The original method is summarized as follows. First, let σ_M be the allowed maximum core width. The attempt is to split a parent vortex of a core width σ_p and strength Γ_p into M thin child vortices, whenever σ_p is greater than σ_M. The widths of the child vortices are selected to be $\alpha\sigma_\mathrm{p}$ with $0 < \alpha < 1$. The larger the α, the smaller the induced splitting error, however but the fatter child vortices are obtained, the sooner child vortices themselves must split.

In Rossi's original scheme, these child vortices are uniformly distributed around the centre of the parent vortex at a distance r away. The value of r and the strength (Γ_c) of the child vortices are determined by preserving the total circulation and the second moment of vorticity about the centre of the parent vortex, where the nth moment is defined as

$$n\text{th moment} \equiv \int (\mathbf{x}\times)^n \boldsymbol{\omega}\, \mathrm{d}x\, \mathrm{d}y \tag{8}$$

This scheme will be called the splitting method (I) hereafter. A careful examination of the induced vorticity field error however reveals that the maximum error always occurs at the centre of the parent vortex and cannot be reduced by increasing the number of child vortices (M). Shiels [26] suggested that instead of preserving the second moment, the vorticity value at the centre of the parent vortex should be preserved. (This scheme is denoted as the splitting scheme (II).) Accuracy is therefore improved.

Table I. Formulae that determine the location and strengths of the M child vortices as well as the thinned parent vortex, if exists.

	Location	Strength
(I)	$r^2/\sigma_p^2 = 1 - \alpha^2$	$\Gamma_c = \Gamma_p/M$
(II)	$r^2/\sigma_p^2 = -\alpha^2 \ln \alpha^2$	$\Gamma_c = \Gamma_p/M$
(III)	$r^2/\sigma_p^2 = 1 - \exp(-r^2/\alpha^2\sigma_p^2)$	$\Gamma_0 = \Gamma_p - M\Gamma_c$ $\Gamma_c = (1 - \alpha^2)\Gamma_p/M \cdot \sigma_p^2/r^2$
(IV)	$r^2/\sigma_p^2 = 2(1 - \alpha^2)$	$\Gamma_0 = \Gamma_p/2$ $\Gamma_c = \Gamma_p/2M$

Since it is the viscosity that causes the growth of the core width, splitting arising from the growth must reflect the truth of diffusion. As far as diffusion is concerned, the parent vortex throws out some but not all of its circulation to the child vortices. Therefore, a physically reasonable layout after splitting should be a thinned and weakened parent vortex surrounded by several child vortices. A new splitting method is thus proposed and described as follows. Let σ_0 and Γ_0 be the width and strength of the parent vortex after splitting. For simplicity, $\sigma_0 = \alpha\sigma_p$ is chosen. Two degrees of freedom r and Γ_0 can now be employed to preserve both the second moment and the vorticity value at the parent's location (denote this scheme as the splitting scheme III). As far as moments are concerned, these degrees of freedom may be alternatively determined by preserving the second and the fourth moments of vorticity (denoted as the splitting scheme IV).

The equations governing the locations and strengths of the child vortices in the above four splitting schemes are summarized in the Table I. The relation between the ratio of r/σ_p and the splitting parameter α is shown in Figure 1. Given a value of α, the splitting schemes (I) and (II) have smaller ratios of r/σ_p because these ratios are used not only to place child vortices but also to maintain most vorticity at the parent's location. Shown in Figure 2 is the induced maximum field error against M in a single splitting event in which $\sigma_p = 1$, $\Gamma_p = \pi$, and $\alpha = 0.9$. As seen, Rossi's scheme (I) has an error independent of M. The other schemes have decreasing errors with an increasing M but the decrease gets saturated quickly. With a fixed $M = 6$, the maximum field errors are again measured and plotted against $(1 - \alpha^2)$ also in Figure 2. As seen, the schemes become third-order accurate in $(1 - \alpha^2)$ with the survival of the parent vortex. Surprisingly, if a smaller M is employed, the order of accuracy becomes smaller too. However, splitting methods (III) and (IV) are always superior to methods (I) and (II).

When there are many fat vortices being split at the same time, the induced errors may be destructive or constructive. Also, errors may accumulate as time goes by. The schemes are next examined by applying them to simulate a decaying Burgers vortex. The initial flow consists of a single vortex element that has a core width of 0.4 and a circulation of 5. The exact vorticity field at time t is known to be

$$\omega(\mathbf{x}, t) = \frac{5}{\pi(0.16 + 4\nu t)} \exp\left(-\frac{|\mathbf{x}|^2}{(0.16 + 4\nu t)}\right) \tag{9}$$

The maximum field errors of numerical solutions with $\nu = 0.04$ at $t = 0.9$ under the choices of $\sigma_M = 0.4$ and $M = 6$ are measured and plotted against $(1-\alpha^2)$ in Figure 3. Two conclusions can

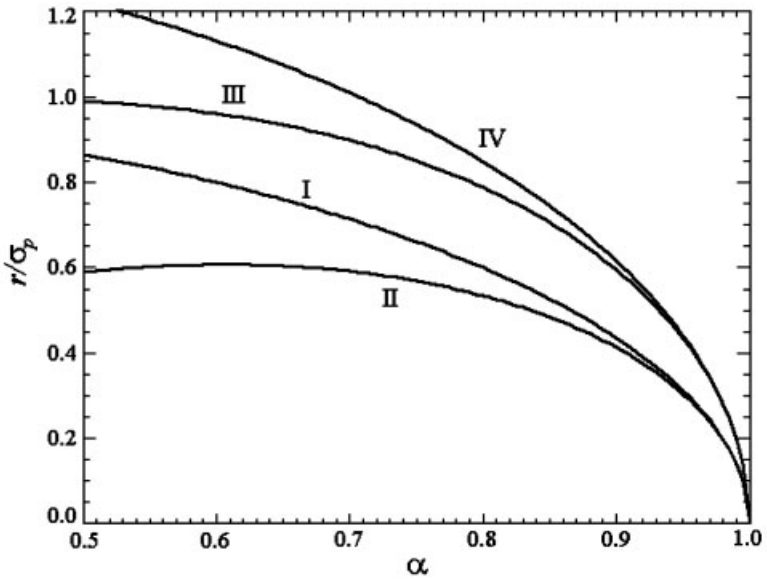

Figure 1. The ratio of the distance r to the original parent's core width (σ_p) versus the splitting parameter α.

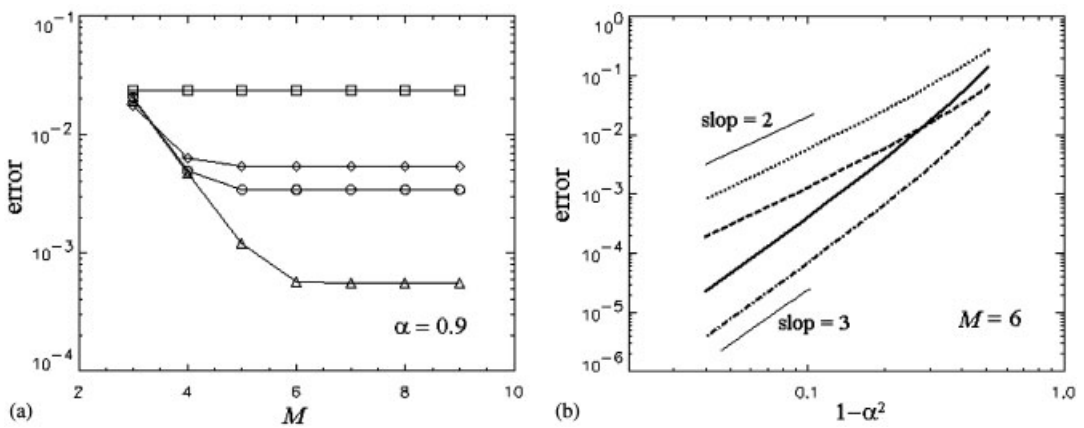

Figure 2. The maximum splitting errors induced in a splitting event: (a) square: I, diamond: II, triangle: III, and circle: IV; and (b) dotted line: I, dash line: II, dash–dotted line: III, and solid line: IV.

be made. First, the newly proposed schemes (III and IV) are capable of reducing the maximum field error by one order of magnitude. Second, errors are constructed or accumulated in the worst way in scheme (II), although it performs better than scheme (I) in a single splitting event.

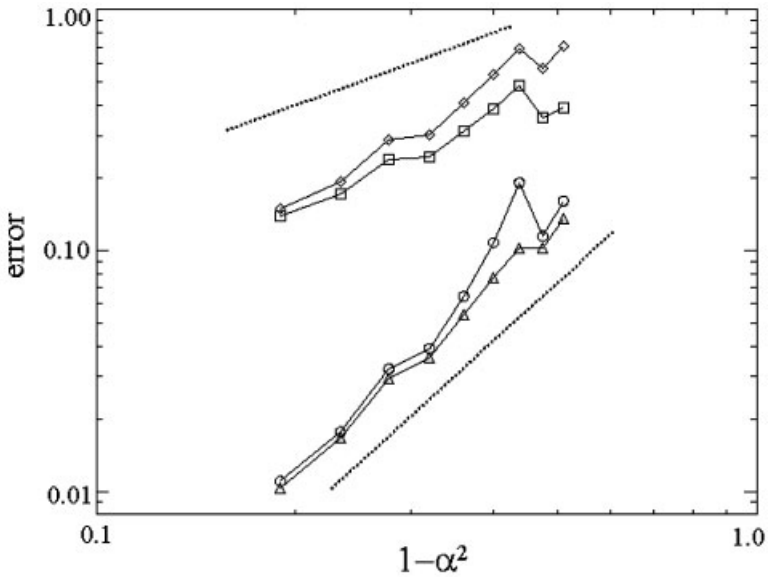

Figure 3. The maximum field errors in simulating a decaying Burgers vortex: square: I; diamond: II; triangle: III; circle: IV. Two dotted lines have slopes of 1 and 2.5 for reference.

2.3. *Merging schemes*

After many splitting events, vortex clusters may be formed and become unnecessarily dense. In order to reduce the computational amount, similar and close-by vortex elements should be merged into one. The first merging scheme was designed by Rossi in 1997 [22] and is described below. Let $\{\Gamma_j, \mathbf{x}_j, \sigma_j\}_{j=1}^{M}$ be the vortices to be merged and $\{\Gamma_0, \mathbf{x}_0, \sigma_0\}$ the resulting vortex. Rossi showed that the induced maximum field error is no greater than $M_1\Gamma_0/\pi\sigma_0^2$, where M_1 is the maximum absolute value of the following function

$$\exp(-x^2) - \beta \exp(-\beta(x-a)^2) \tag{10}$$

in the parameter domain of $b_1 \leqslant \beta = \sigma_0^2/\sigma_j^2 \leqslant b_2$ and $a = |\mathbf{x}_j - \mathbf{x}_0|/\sigma_0 \leqslant R$. In Rossi's scheme, b_1, b_2, and R are prescribed and M_1 is found in advance. A merging event is claimed to succeed only if every pair of (β, a) in the group of vortices lies within the prescribed parameter domain and if the upper bound of the merging error, $M_1\Gamma_0/\pi\sigma_0^2$, is less than some error tolerance. If any of these criteria is not fulfilled, merging is not allowed and all the related computations become useless and wasted. To improve this shortcoming, one notices that the upper bound of the induced error can be replaced by $\Gamma_0/\pi \operatorname{Min}_{1\leqslant j\leqslant M} \sigma_j^2$, if $\sigma_0^2/\sigma_j^2 > 1$ for some j. This comes from the observation that $M_1 = \operatorname{Max}(1, \beta)$ for an arbitrary a. Let $\varepsilon\Gamma$ be the error tolerance, where Γ is a referenced circulation (for example, the total circulation of a flow). Then the merging criterion becomes

$$\Gamma_0/\Gamma < \pi\varepsilon \operatorname*{Min}_{1\leqslant j\leqslant M} \sigma_j^2 \tag{11}$$

Consequently, after the group of vortices, $\{\Gamma_j, \mathbf{x}_j, \sigma_j\}_{i=1}^{M}$, is selected, σ_0 is not computed unless criterion (11) is fulfilled. A successful merging event is claimed only if σ_0 is computed and $\sigma_0 \leqslant \sigma_M$.

To determine $\{\Gamma_0, \mathbf{x}_0, \sigma_0\}$, Rossi suggested the restrictions of preserving the total circulation, the first and the second moments of vorticity. Consequently,

$$\Gamma_0 = \sum_{j=1}^{M} \Gamma_j \tag{12}$$

$$\Gamma_0 \mathbf{x}_0 = \sum_{j=1}^{M} \Gamma_j \mathbf{x}_j \tag{13}$$

$$\Gamma_0 \sigma_0^2 = \sum_{j=1}^{M} \Gamma_j (\sigma_j^2 + |\mathbf{x}_j - \mathbf{x}_0|^2) \tag{14}$$

Luckily, the condition that $\sigma_0^2/\sigma_j^2 > 1$ for some j is guaranteed from Equation (14) if all vortices rotate in a same direction. This merging scheme will be labeled as the merging scheme (a) in the present study. Alternatively, if one prefers, Equation (14) may be replaced by

$$\frac{\Gamma_0}{\sigma_0^2} = \sum_{j=1}^{M} \frac{\Gamma_j}{\sigma_j^2} \exp\left(-\frac{|\mathbf{x}_j - \mathbf{x}_0|^2}{\sigma_j^2}\right) \tag{15}$$

which preserves the vorticity value at $\mathbf{x}_0$. This is the merging scheme (b). If all vortices rotate in the same direction, say in the counterclockwise direction, then it is obvious that

$$\frac{\Gamma_0}{\sigma_0^2} \leqslant \sum_{j=1}^{M} \frac{\Gamma_j}{\sigma_j^2} \leqslant \frac{\sum_{j=1}^{M} \Gamma_j}{\mathrm{Min}_{1 \leqslant j \leqslant M}\ \sigma_j^2}$$

Consequently, it is guaranteed again that $\sigma_0^2/\sigma_j^2 > 1$ for some j.

Finally, in either method, σ_0 cannot be calculated until the group of vortex elements to be merged has been selected. Moreover, if two far-away vortices are merged, the resulting σ_0 is easily larger than σ_M and becomes unwanted. In the present work, an algorithm modified from Rossi's original one is used. Its procedures are listed below:

1. Select the referenced circulation Γ and specify the error tolerance ε.
2. Loop on i from 1 to N. Set C consisting of i.
3. Loop on j from $i+1$ to N. Element j is added to C if $\Gamma_i \cdot \Gamma_j > 0, |\mathbf{x}_j - \mathbf{x}_i| \leqslant \eta\sigma_M$, and so far the total circulation in C is less than $\Gamma_{\mathrm{ref}} = \pi\varepsilon(\alpha\sigma_M)^2\Gamma$.
4. End loop j.
5. If $|C| > 1$, find the minimum σ_j^2 and compute Γ_0.
6. If $\Gamma_0/\Gamma \leqslant \varepsilon\pi\,\mathrm{Min}_{1 \leqslant j \leqslant M}\,\sigma_j^2$, compute $\mathbf{x}_0$ and σ_0.
7. If $\sigma_0 \leqslant \sigma_M$, replace $\{\Gamma_i, \sigma_i, \mathbf{x}_i\}$ by $\{\Gamma_0, \sigma_0, \mathbf{x}_0\}$ and remove all the other vortices in C from the simulation.
8. End loop i.

Note that the parameter η is introduced in the algorithm to avoid selecting too far-away vortices. Also, because the minimum core width is expected to be about $\alpha\sigma_M$, the referenced

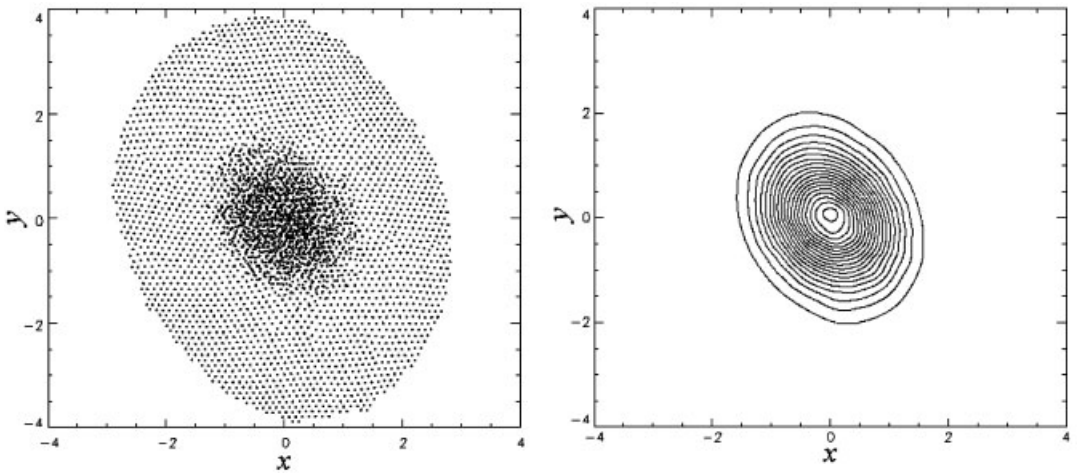

Figure 4. The locations of the computational vortex elements and the vorticity contours (ω) at the last simulation time $\tau = 2$.

circulation Γ_{ref} is chosen. Finally, because simulations with lots of splitting events are targeted, the merging procedures are carried out at time steps when splitting events occur. Temporarily huge computational amount can thus be avoided.

The validity of the proposed merging schemes is now tested as follows. Consider the evolution of a Burgers vortex of radius 1 and a circulation 20π under an external straining field $\mathbf{U}_S = (-\alpha x, -\beta y, \gamma z)$ with $\alpha = 1$, $\beta = 3$, and $\gamma = 4$. A non-axisymmetric steady state is expected. To simulate such a flow, a coordinate transformation is needed and will be described later in the next section. The fluid viscosity v is taken to be one and thus the associated Reynolds number $Re = \Gamma/2\pi v$ is 10. The instantaneous locations of the computational vortex elements and the nearly steady vorticity contours (ω) at the last simulation time $\tau = 2$, obtained using the method (IIIb) with $M = 6$, $\alpha = 0.9$, $\sigma_M = 0.3$, and a time increment $\mathrm{d}\tau = 0.001$ are shown in Figure 4. The error tolerance for merging is chosen to be $\varepsilon = 0.01/(1 + \gamma\tau)$. The evolutions of the second principal moments, σ'_x and σ'_y, of vorticity are plotted against the simulation time τ in Figure 5. The values are asymptotic to those (0.86 and 1.23 as marked by arrows in the figure) obtained by Robinson and Saffman [24].

The accuracies of the numerical solutions can be further examined by measuring the steady vorticity value at the origin, which is found herein by averaging the vorticity values at the origin over the last 500 time steps. They are $\omega/2Re = 0.962$ (IIIa) and 0.971 (IIIb) when $\sigma_M = 0.5$, and they are 0.952 (IIIa) and 0.954 (IIIb) as $\sigma_M = 0.3$, compared to 0.95 obtained by Robinson and Saffman [24] and 0.953 by Buntine and Pullin [25]. In all simulations addressed, the merging scheme, (a) or (b), works successfully in controlling the total number of the computational vortex elements for such a long time simulation. The number is about 4000 when $\sigma_M = 0.5$ and about 10 000 when $\sigma_M = 0.3$ at the last simulation time $\tau = 2$. Finally, it should be mentioned that the core-spreading vortex method without a splitting technique generates totally wrong results for the present problem. Nearly axisymmetric flows are obtained instead, because the core widths become too large eventually.

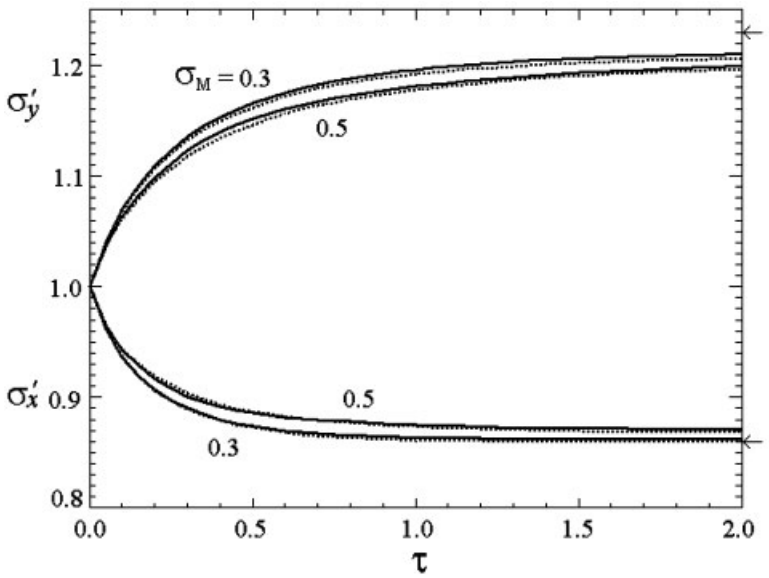

Figure 5. The evolutions of the principal second moments of a strained Burgers vortex: solid lines: IIIa; dotted lines: IIIb.

The above merging scheme however only allows merging vortex elements of a same rotation. From the viewpoint of remeshing, merging elements of opposite rotations is not unreasonable as long as it does not induce errors larger than the given tolerance. As studied by Rossi [22], the field error induced in a merging event, $E(\mathbf{x})$, is

$$E(\mathbf{x}) = \left| \frac{\Gamma_0}{\pi\sigma_0^2} \exp\left(-\frac{|\mathbf{x}-\mathbf{x}_0|^2}{\sigma_0^2}\right) - \sum_j \frac{\Gamma_j}{\pi\sigma_j^2} \exp\left(-\frac{|\mathbf{x}-\mathbf{x}_j|^2}{\sigma_j^2}\right) \right|$$

$$= \left| \sum_j \frac{\Gamma_j}{\pi\sigma_0^2} \left\{ \exp\left(-\frac{|\mathbf{x}-\mathbf{x}_0|^2}{\sigma_0^2}\right) - \frac{\sigma_0^2}{\sigma_j^2} \exp\left(-\frac{|\mathbf{x}-\mathbf{x}_j|^2}{\sigma_j^2}\right) \right\} \right|$$

It is easy to show that

$$E(\mathbf{x}) \leqslant \sum_j \frac{|\Gamma_j|}{\pi\sigma_0^2} \cdot M_1 \tag{16}$$

where as before M_1 is the maximum absolute value of function (10). The merging criterion therefore must be changed to

$$\sum_j \frac{|\Gamma_j|}{\pi\sigma_0^2} \cdot M_1 < \varepsilon\Gamma_{\text{ref}}$$

Furthermore, two more restrictions are needed if the extension of the above merging scheme to merge vortex elements of opposite rotations is required. First, because there is now no

guarantee that σ_0 is greater than σ_j for some j, one has to check whether $\sum_j|\Gamma_j|/\Gamma \leqslant \varepsilon\pi\sigma_0^2$. Second, the conservation of the first moment, Equation (13), may result in a far, irrational, location $\mathbf{x}_0$. A criterion $\mathrm{Max}_{1\leqslant j\leqslant M}|\mathbf{x}_0 - \mathbf{x}_j| \leqslant \eta\sigma_M$ is thus added and examined after $\mathbf{x}_0$ is computed and before σ_0 is computed. Finally, the restriction that $\Gamma_i \cdot \Gamma_j > 0$ in step 3 is no longer needed. Merging is given up as soon as any of the criteria is not fulfilled. Such a merging scheme will be verified in the next section.

3. ILLUSTRATIONS

To verify the proposed splitting and merging methods, the attempt is to simulate the interactions between two Burgers vortices under an external straining field. These kinds of flows were first analysed by Robinson and Saffman [24] in use of the perturbation method and simulated by Buntine and Pullin [25] by a spectral method. The flow is briefly introduced now. Consider a velocity field $\mathbf{u} = \mathbf{U}_S + \boldsymbol{\upsilon}$, where $\mathbf{U}_S$ is incompressible as well as irrotational and $\boldsymbol{\upsilon}(x, y, t)$ is two dimensional. The straining field $\mathbf{U}_S$ is selected to be $\mathbf{U}_S = (-\alpha x, -\beta y, \gamma z)$ with $\gamma = \alpha + \beta$. It can be shown that the vorticity ω is governed by

$$\frac{\partial\omega}{\partial t} + u\frac{\partial\omega}{\partial x} + \upsilon\frac{\partial\omega}{\partial y} = \gamma\omega + \nu\left(\frac{\partial^2\omega}{\partial x^2} + \frac{\partial^2\omega}{\partial y^2}\right) \tag{17}$$

Under the transformation of

$$\Omega(X, Y, \tau) = \omega(x, y, t)\mathrm{e}^{-A(t)} = \frac{\partial V}{\partial X} - \frac{\partial U}{\partial Y} \tag{18}$$

$$\tau = \int_0^t \mathrm{e}^{A(t)}\,\mathrm{d}t \tag{19}$$

$$(X, Y) = (x, y)\mathrm{e}^{A(t)/2} \tag{20}$$

and

$$A(t) = \int_0^t \gamma(t)\,\mathrm{d}t \tag{21}$$

it is known that Equation (17) can be rewritten as

$$\frac{\partial\Omega}{\partial\tau} + (U - \lambda X)\frac{\partial\Omega}{\partial X} + (V + \lambda Y)\frac{\partial\Omega}{\partial Y} = \nu\left(\frac{\partial^2\Omega}{\partial X^2} + \frac{\partial^2\Omega}{\partial Y^2}\right) \tag{22}$$

where $\lambda = (\beta - \gamma/2)/\exp A$. It is the vorticity field $\Omega(X, Y, \tau)$ that will be solved by the present vortex methods. Vortex elements are now set to move at a velocity of $(U - \lambda X, V + \lambda Y)$. The evolution of the vorticity field ω however is going to be discussed.

Experiences show that the splitting method (II) often works poorly and thus is discarded. For consistency, combinations of splitting and merging schemes like (Ia) and (IVa) will be employed. Combinations like both (IIIa) and (IIIb) are of interest.

3.1. Merging of two Burgers vortices of a same rotation

The goal is to obtain the complete merging process of two Burgers vortices which have a radius $a=1$ and are separated by a distance of $d=4$. The external straining field has $\gamma=4$ and $\beta=3$. The fluid viscosity is $v=1$. Each of the Burgers vortices is initially discretized into 222 vortex elements uniformly distributed along 8 concentric circles as shown in Figure 6. They all have an initial core width of $\sigma_j(0)=0.25$. Their strengths are so adjusted that the vorticity values are exact at their locations, except those elements in the most outer circle. The strengths of those elements are adjusted to match the desired Reynolds number $Re=\Gamma/2\pi v=80$, where Γ is the circulation of one Burgers vortex. The simulation parameters used are $\alpha=0.85$, $M=4$, $\sigma_M=0.325$, $\varepsilon=0.0002$, $\eta=0.5$, and $\mathrm{d}\tau=0.001$, under the consideration of both the accuracy and the efficiency. The first splitting event is thus expected to occur at $\tau_1=(\sigma_M^2-\sigma(0)^2)/4v\approx 0.011$. The time period between two successive splitting events is $\Delta\tau=\sigma_M^2(1-\alpha^2)/4v\approx 0.0073$. The three important time scales involved in this flow are respectively the convective timescale $t_\Gamma=2\pi d^2/Re$, the straining timescale $t_\gamma=4\gamma^{-1}$, and the viscous timescale $t_v=a^2/v$. The latter two have been normalized to be one [25].

Figure 6 shows the so-obtained merging process at some selected times. The results agree well with those obtained by Buntine and Pullin [25]. Nearly the same results are obtained as well when the resolution is increased to be $\sigma_M=0.25$ (not shown here). A too large σ_M however causes the flow to be too diffusive. Physically it should not be greater than the length scale $\sqrt{v/\gamma}=0.5$. The accuracies of the schemes are compared by the computed radial vorticity distributions as shown in Figure 7. Compared to the results ($\theta=0^\circ$) of Buntine and Pullin, schemes (IIIb) and (IVa) seemingly have the best agreement; (Ia) slightly overpredicts while (IIIa) slightly underpredicts the vorticity value at the origin. The difference however is not much, probably because the merging errors dominate over the splitting errors.

The numbers of the computational vortex elements are about the same for the four schemes as shown in Figure 8 and are much smaller than the grid number (128^2) used by Buntine and Pullin [25]. The numbers increase approximately linearly in time τ because of the spatial transformation, Equation (20). That is, because the area with non-negligible vorticity grows linearly in $(1+\gamma\tau)$, so does the number of the computational vortex elements. In remark, the proposed splitting and merging schemes successfully and efficiently simulate the interaction between two Burgers vortices of a same rotation.

3.2. Cancellation of two Burgers vortices of opposite rotations

At last, the proposed schemes are applied to the simulation of the cancellation of two Burgers vortices of opposite rotations. The external straining field with $\beta=16$ and $\gamma=4$ is chosen. The initial condition is the same as that in the previous subsection except that the right Burgers vortex is changed to be clockwise. For simplicity, the centre of the external straining field is chosen to move vertically together with the centre, $\mathbf{x}_c$, of the Burgers vortex. The y-displacement of the vortex centre is obtained by solving

$$\frac{\mathrm{d}y_c}{\mathrm{d}t}=v(x_c,y_c,t),\quad y_c(0)=0 \tag{23}$$

or after transformation

$$\frac{\mathrm{d}Y_c}{\mathrm{d}\tau}=V(X_c,Y_c,\tau)+\frac{\gamma Y_c}{2(1+\gamma\tau)},\quad Y_c(0)=0 \tag{24}$$

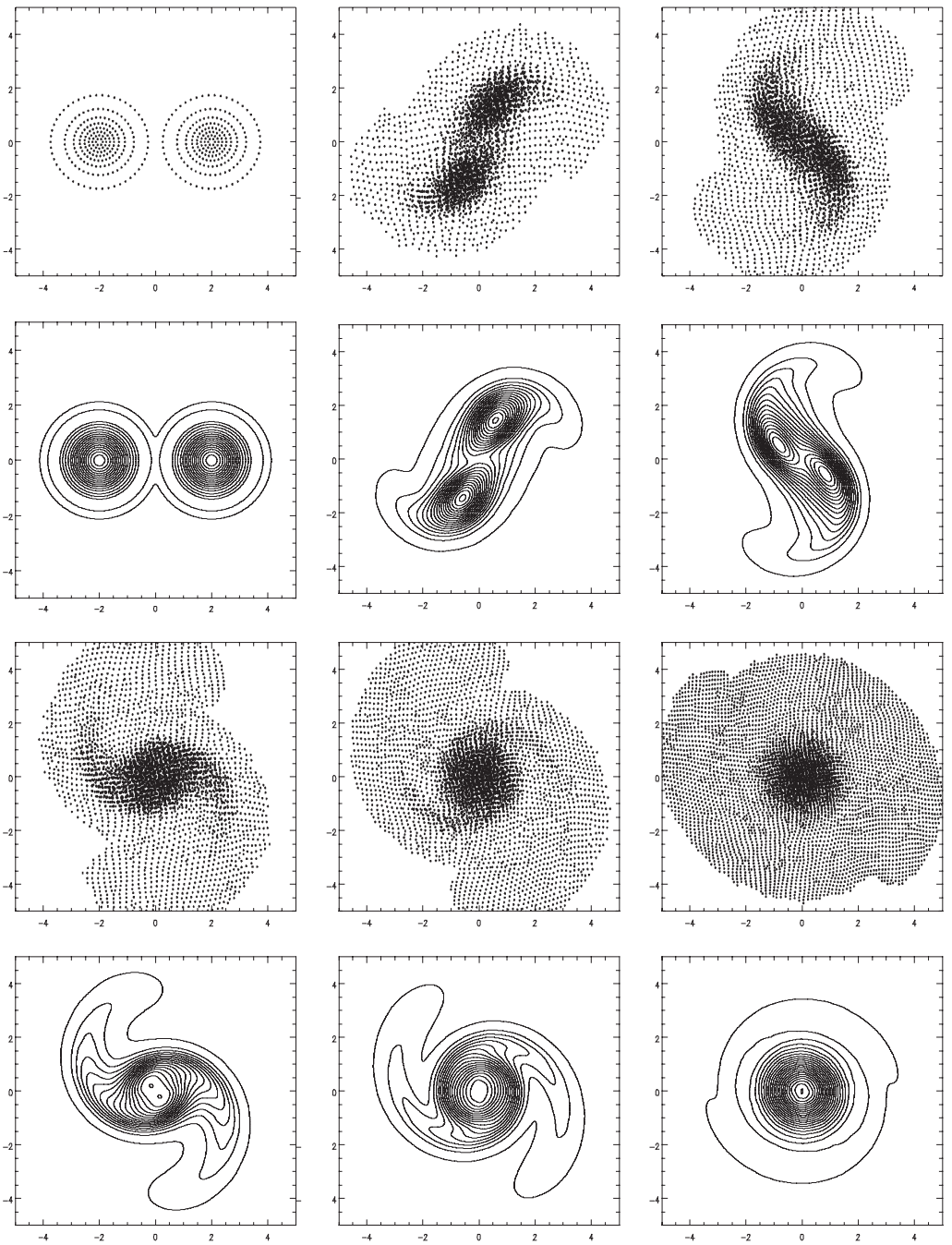

Figure 6. The merging process as $Re = 80$ obtained by scheme (IVa). The instantaneous locations of the vortex elements and the vorticity contours ($\Delta\omega = 9$ and $\omega_{\min} = 1$) at $\tau(t) = 0(0)$, 0.1(0.08),0.2(0.15),0.3(0.20),0.4(0.24), and 0.8(0.36) are shown.

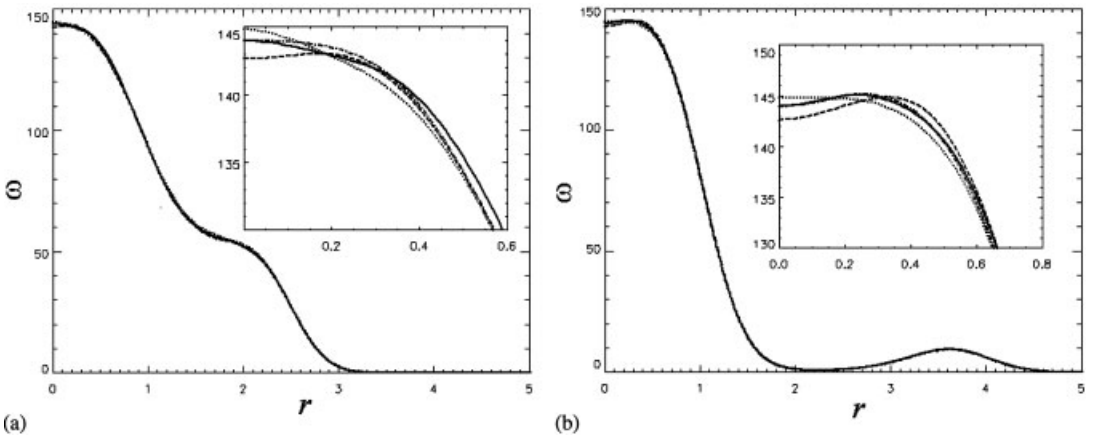

Figure 7. The radial distributions of the vorticity along the directions: (a) $\theta = 0°$; and (b) $\theta = 115°$ at $t = 0.2$. Dotted line: Ia; Dash line: IIIa; Dash dotted line: IIIb; Solid: IVa.

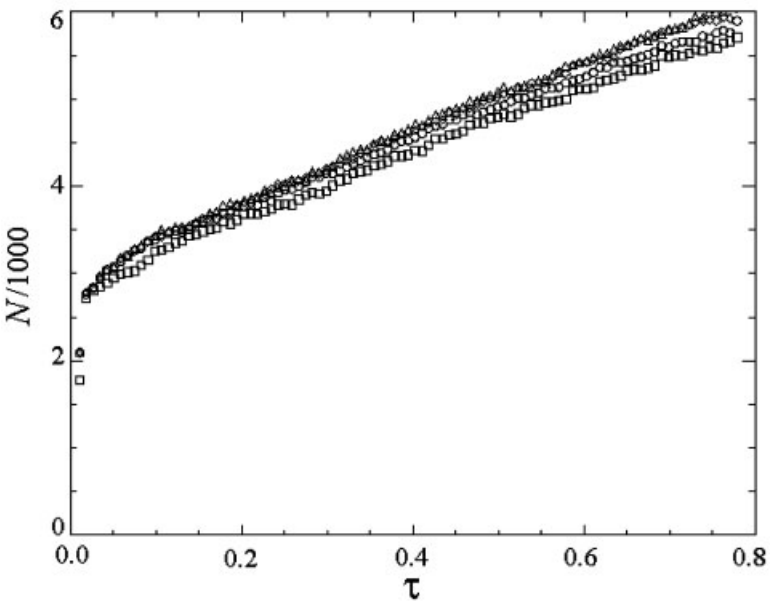

Figure 8. The numbers of the employed computational vortex elements at every other $\Delta\tau$: squares: Ia, triangles: IIIa; diamonds: IIIb; and circles: IVa.

The velocities of the computational vortex elements are also changed correspondingly to become $(U - \lambda X, V + \lambda Y - \lambda_c Y_c)$, where $\lambda_c = (\beta - \gamma)/(1 + \gamma\tau)$, and to save computations, the vortex elements running below $y_c - 25$ will be discarded.

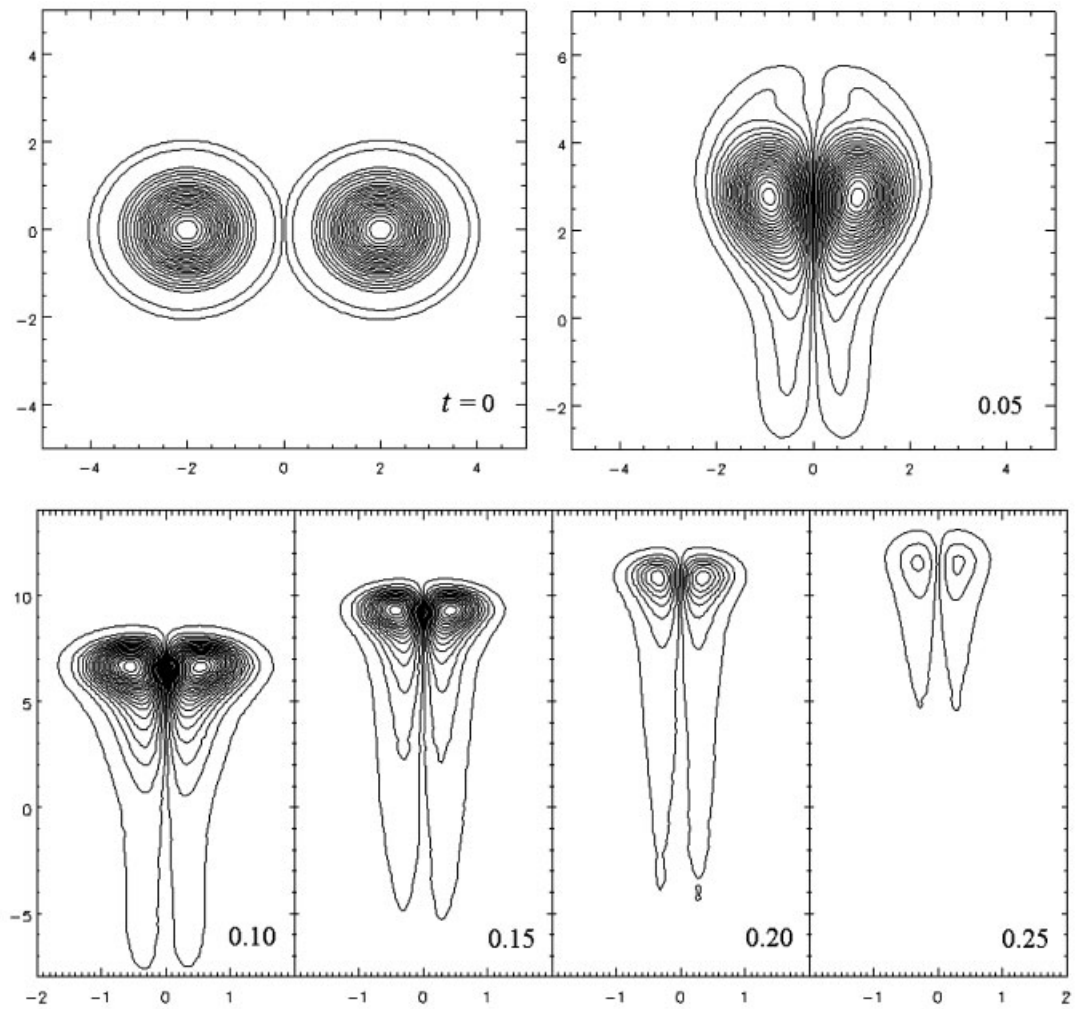

Figure 9. The vorticity contours ($|\omega_{\min}| = 5, |\Delta\omega| = 15$) during the cancellation obtained by scheme(IIIb).

The simulation parameters employed are $\alpha = 0.85$, $M = 4$, $\sigma_M = 0.325$, $\eta = 0.5$ and $d\tau = 0.0005$. On the other hand, because the circulation of each of the two Burgers vortices decays exponentially like $\exp(-\beta t)$ at large times [25], the error tolerance is chosen to be $\varepsilon = \varepsilon_0$ for $t \leqslant t_0$ and $\varepsilon = \varepsilon_0 \exp(-\beta(t - t_0))$ for $t > t_0$ with $\varepsilon_0 = 0.005$ and $\beta t_0 = 2$. Figure 9 shows the so-obtained cancellation process with $Re = 160$ from the scheme (IIIb). The results are reasonably well, although slightly more diffusive than those observed in the Figure 16 of Buntine and Pullin [25]. Figure 10 shows the residuary circulation on a half-plane and the y-displacement of the vortex centre against βt. As seen, all schemes give close results that agree well with the previous investigation. In the moving frame, the centre moves upward at early times at a

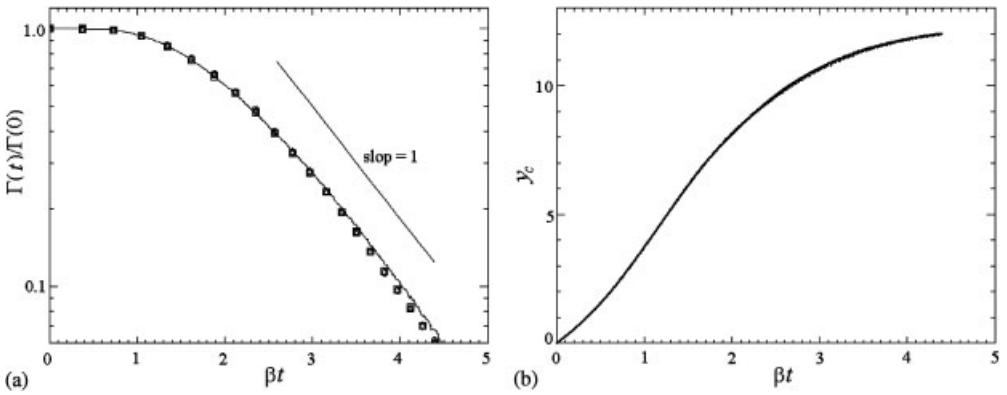

Figure 10. (a) The residuary circulation $\Gamma(t)$ against βt: square: Ia; triangle: IIIa; diamond: III(b); circle: IVa; and (b) the y-displacement of the vortex centre against βt: dotted: Ia; dash: IIIa; dash dotted: III(b); solid: IVa. The solid curve in (a) is the residuary circulation extracted from Figure 18 of Buntine and Pullin [25].

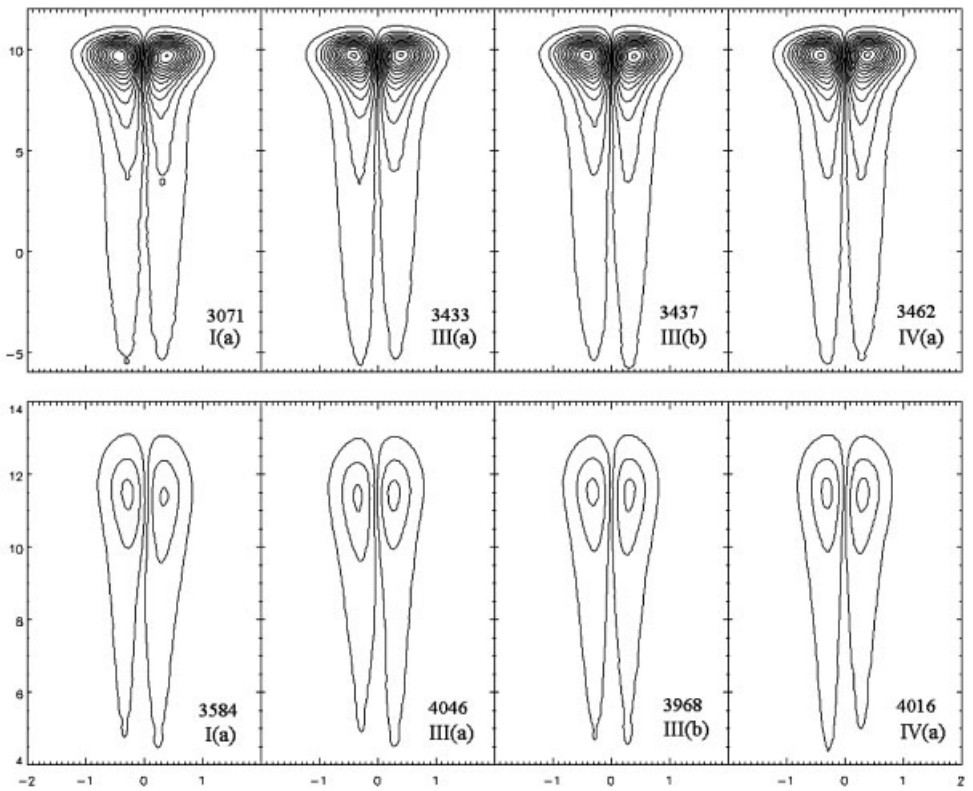

Figure 11. The vorticity contours at $t = 0.16$ and 0.25. The minimum contour is $|\omega_{\min}| = 5$ and all contour intervals are $|\Delta\omega| = 15$. The numbers labeled are those of the computational vortex elements in use.

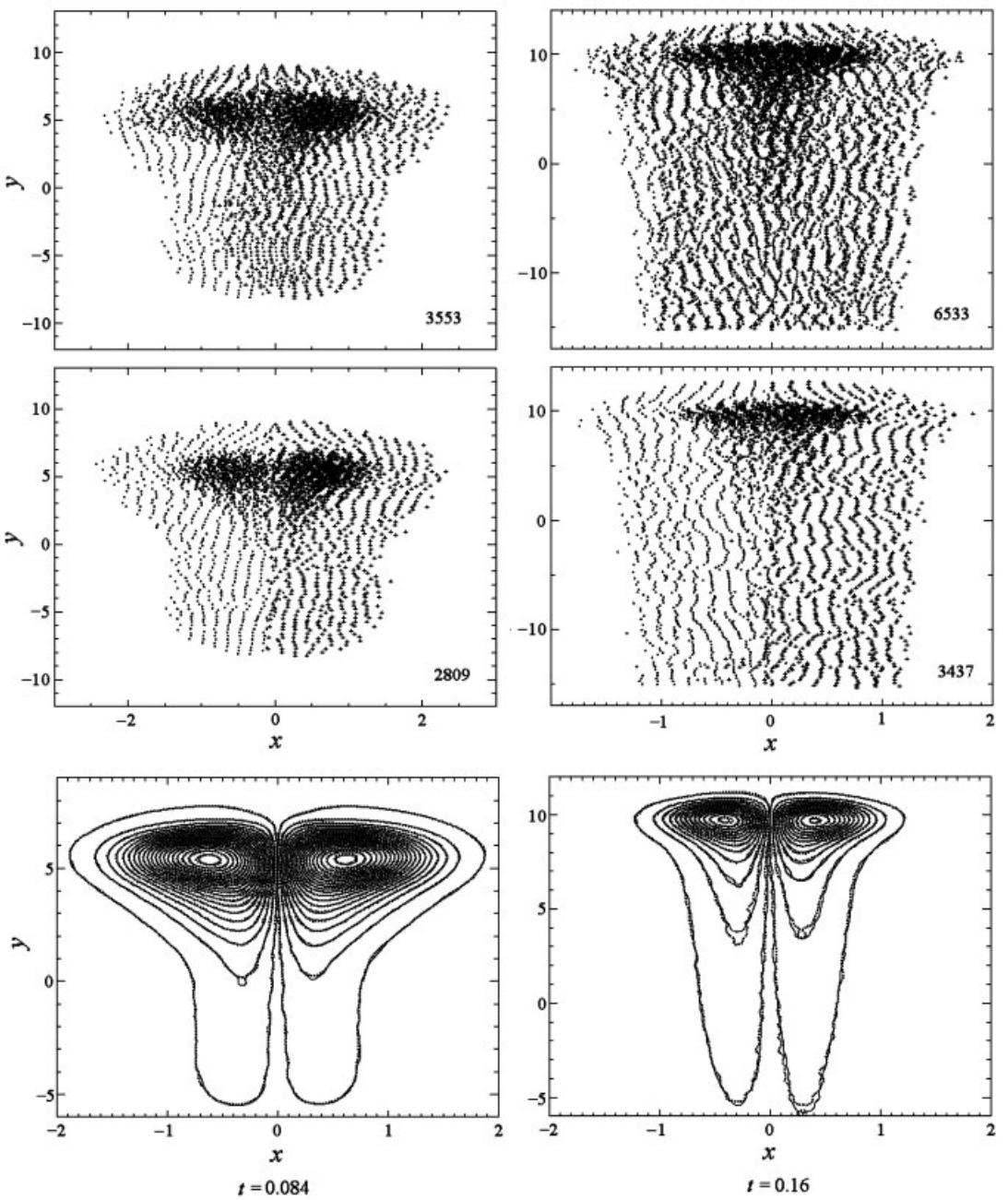

Figure 12. The locations of the counterclockwise (•) and clockwise (+) vortex elements and the vorticity contours at time $t = 0.084$ and 0.16 from IIIb with (solid) and without (dotted) merging vortex elements of opposite rotations. The minimum contour is $|\omega_{\min}| = 5$ and all contour intervals are $|\Delta\omega| = 15$.

speed equal to $\Gamma/2\pi d$. The movement gradually slows down as the time increases, because of the exponential decay of the residuary circulation.

To distinguish the schemes under investigation, the vorticity contours at $t = 0.16$ and $t = 0.25$ are presented in Figure 11 for comparison. The total numbers of the computational vortex elements are also indicated. Among all, scheme (Ia) performs worst; (IIIb) and (IVa) perform better than (IIIa). Although the simulated flows are not perfectly symmetric because of the index dependence of the merging algorithm, simulation results with the permission of merging elements of opposite rotations are seemingly encouraging. The instantaneous locations of the counterclockwise ($\bullet$) and clockwise ($+$) vortex elements at $t = 0.084$ and 0.16 from results obtained by the scheme (IIIb), with or without a permission to merge elements of opposite rotations are shown in Figure 12. As seen, the clockwise (counterclockwise) vortex elements are gradually 'diffused' through splitting to the left (right) half-plane. The permission of merging elements of opposite rotations significantly reduces the total number of the computational elements (nearly by half at larger times) and most of all, harms the accuracy little.

4. CONCLUSIONS

A new vortex splitting method to simulate diffusion has been proposed. In the new splitting method, the parent vortex (the vortex element to be split) is retained after splitting, but its core width and strength are both shrunk. For convenience, the shrunk core width is chosen to be the same as that of the surrounding child vortex elements. Its strength, on the other hand, is determined by preserving either the moments of vorticity and/or the vorticity value at its location. About half circulation is thus retained in the parent vortex and the remaining is 'diffused' to the surrounding child vortices. The splitting error can thus be reduced by one order of magnitude. To control the total number of the computational vortex elements, Rossi's merging scheme is employed and modified in a way such that less restrictions are required and merging vortex elements of opposite rotations is allowed.

The proposed schemes are verified by applying them to the simulations of interactions between two Burgers vortices of same or opposite rotations under external straining fields. Reasonably good results are obtained with reasonably many of the computational vortex elements. Experiences suggest that the maximum allowable core width and the error tolerance for merging close-by and similar vortices dominate the error. The smaller these two factors, the higher the accuracy, but the more computational vortex elements are needed. In addition, the CPU time spent in merging vortex elements is more than that spent in splitting. Both however are less than the CPU time spent in computing the Biot–Savart velocities. An index-independent and faster merging algorithm is under development by employing the cell concept used in the direction-simulation Monte-Carlo (DSMC) method.

ACKNOWLEDGEMENTS

The support of this work by the National Science Council, Taiwan, under the contract NSC 91-2212-E-002-092 is gratefully acknowledged.

REFERENCES

1. Leonard A. Vortex methods for flow simulations. *Journal of Computational Physics* 1980; **37**:289–335.
2. Chang C, Chern R. A numerical study of flow around an impulsively started circular cylinder by a deterministic vortex method. *Journal of Fluid Mechanics* 1991; **233**:243–263.
3. Lu ZY, Shen SF. In *Numerical Methods in Laminar and Turbulent Flow*, Taylor C *et al.* (eds), vol. 5. Pineridge Press: Swansea, U.K., 1987; 619.
4. Lu ZY, Ross TJ. Diffusing-vortex numerical scheme for solving incompressible Navier–Stokes equations. *Journal of Computational Physics* 1991; **95**:400–435.
5. Greengard C. The core-spreading vortex method approximations the wrong equation. *Journal of Computational Physics* 1985; **61**:345–348.
6. Chorin AJ. Numerical study of slightly viscous flow. *Journal of Fluid Mechanics* 1973; **57**:785–796.
7. Degond P, Mas-Gallic S. The weighted particle method for convection–diffusion equations. Part 1: the case of an isotropic viscosity. *Mathematics of Computation* 1989; **53**:485–507.
8. Fishelov D. A new vortex scheme for viscous flow. *Journal of Computational Physics* 1990; **86**:211–224.
9. Shankar S, Van Dommelen LL. A new diffusion procedure for vortex methods. *Journal of Computational Physics* 1996; **127**:88–109.
10. Van Dommelen LL, Shankar S. Two counter-rotating diffusing vortices. *Physics of Fluids A* 1995; **7**:808–819.
11. Ogami Y, Akamatsu T. Viscous flow simulation using the discrete vortex model—the diffusion velocity method. *Computers and Fluids* 1991; **19**:433–441.
12. Kempka SN, Strickland JH. A method to simulate viscous diffusion of vorticity by convective transport of vortices at a non solenoidal velocity. *Sandia Lab Report SAND93-1763*, 1993.
13. Shintani M, Akamatsu T. Investigation of two dimensional discrete vortex method with viscous diffusion model. *Computational Fluid Dynamics* 1994; **3**:237–254.
14. Huang MJ. Circulation conserved diffusion vortex method. *Transactions of the Aeronautical and Astronautical Society of the Republic of China* 2003; **35**:65–72.
15. Huang MJ, Chen YY. Accuracy of the circulation-conserved diffusion vortex method. *Proceeding of the 10th National Computational Fluid Dynamics Conference*, Hua-Lien, August 2003.
16. Leonard A. Computing three-dimensional incompressible flows with vortex elements. *Annual Review of Fluid Mechanics* 1985; **17**:523–559.
17. Anderson, Greengard. On vortex methods. *SIAM Journal on Numerical Analysis* 1985; **22**:413–440.
18. Gustavson, Sethian. *Vortex Method and Vortex Motion*. SIAM: Philadelphia, PA, 1991.
19. Beale, Cottet, Huberson. *Vortex Flows and Related Numerical Methods*. Kluwer Academic Publishers: Dordrecht, 1993.
20. Cottet, Koumoutsakos. *Vortex Methods*: *Theory and Practice*. Cambridge University Press: Cambridge, 2000.
21. Rossi L. Resurrecting core-spreading vortex methods: a new scheme that is both deterministic and convergent. *SIAM Journal on Scientific Computing* 1996; **17**:370–397.
22. Rossi L. Merging computational elements in vortex simulations. *SIAM Journal on Scientific Computing* 1997; **18**:1014–1027.
23. Rossi LF, Lingevitch JF, Bernoff AJ. Quasi-steady monopole and tripole attractors for relaxing vortices. *Physics of Fluids* 1997; **9**:2329–2338.
24. Robinsin AC, Saffman PG. Stability and structure of stretched vortices. *Studies in Applied Mathematics* 1984; **70**:163–181.
25. Buntine JD, Pullin DI. Merger and cancellation of strained vortices. *Journal of Fluid Mechanics* 1989; **205**: 263–295.
26. Shiels D. Simulation of controlled bluff body flow with a viscous vortex method. *Ph.D. Thesis*, California Institute of Technology, Pasadena, CA, 1998.

